10-22-1999

Beam test results for the FiberGLAST instrument

Robert S. Mallozzi
University of Alabama - Huntsville

R M. Kippen
University of Alabama - Huntsville

Geoffrey N. Pendleton
University of Alabama - Huntsville

W Paciesas
University of Alabama - Huntsville

Georgia A. Richardson
University of Alabama - Huntsville

See next page for additional authors

Recommended Citation

Robert S. Mallozzi ; Richard M. Kippen ; Geoffrey N. Pendleton ; William S. Paciesas ; Georgia A. Richardson ; Surasak Phengchamnan ; Gerald Karr ; Donald B. Wallace ; Gerald J. Fishman ; Thomas A. Parnell ; Robert B. Wilson ; Mark J. Christl ; W. Robert Binns ; Paul L. Hink ; Martin H. Israel ; Keith R. Rielage ; John W. Epstein ; Paul F. Dowkontt ; James H. Buckley ; James M. Ryan ; John R. Macri ; Mark L. McConnell ; Tumay O. Tumer ; Michael L. Cherry ; T. Gregory Guzik ; John G. Stacy ; S. C. Kappadath ; Muzaffer Atac ; Katsushi Arisaka ; David B. Cline and Yuriy Pischalnikov "Beam test results for the FiberGLAST instrument", Proc. SPIE 3765, EUV, X-Ray, and Gamma-Ray Instrumentation for Astronomy X, 22 (October 22, 1999); doi:10.1117/12.366510; http://dx.doi.org/10.1117/12.366510

Authors
Robert S. Mallozzi, R M. Kippen, Geoffrey N. Pendleton, W Paciesas, Georgia A. Richardson, Surasak Phengchamnan, Gerald Karr, Donald B. Wallace, Gerald J. Fishman, Thomas A. Parnell, Robert B. Wilson, Mark J. Christl, W Robert Binns, P L. Hink, Martin W. Israel, Keith R. Rielage, John W. Epstein, Paul F. Dowkontt, J Buckley, James M. Ryan, John R. Macri, Mark L. McConnell, O T. Tumer, M L. Cherry, T G. Guzik, J G. Stacy, S C. Kappadath, Muzaffer Atac, Katsushi Arisaka, David B. Cline, and Yuriy Pischalnikov

Beam test results for the FiberGLAST instrument

R. S. Mallozzi[a], R. M. Kippen[a], G. N. Pendleton[a], W. S. Paciesas[a], G. A. Richardson[a], S. Phengchamnan[a], G. Karr[a], D. Wallace[a], G. J. Fishman[b], T. A. Parnell[b], R. B. Wilson[b], M. J. Christl[b], W. R. Binns[c], P. L. Hink[c], M. H. Israel[c], K. R. Rielage[c], J. W. Epstein[c], P. Dowkontt[c], J. H. Buckley[c], J. M. Ryan[d], J. Macri[d], M. L. McConnell[d], T. O. Tümer[e], M. L. Cherry[f], T. Gregory Guzik[f], J. Gregory Stacy[f], S. C. Kappadath[f], M. Atac[g], K. Arisaka[g], D. Cline[g], Y. Pischalnikov[g]

[a]University of Alabama in Huntsville, Huntsville, AL
[b]NASA/Marshall Space Flight Center, Huntsville, AL
[c]Washington University, St. Louis, MO
[d]University of New Hampshire, Durham, NH
[e]University of California Riverside, Riverside, CA
[f]Louisiana State University, Baton Rouge, LA
[g]University of California Los Angeles, Los Angeles, CA

ABSTRACT

The FiberGLAST scintillating fiber telescope is a large-area instrument concept for NASA's Gamma Ray Large Area Space Telescope (GLAST) program. The detector is designed for high-energy (E $\gtrsim$10 MeV) gamma–ray astronomy, and uses plastic scintillating fibers to combine a photon pair tracking telescope and a calorimeter into a single instrument. A small prototype detector has been tested with high energy photons at the Thomas Jefferson National Accelerator Facility. We report on the results of this beam test, including scintillating fiber performance, photon track reconstruction, angular resolution, and detector efficiency.

Keywords: gamma-rays, astronomy, instrumentation

1. INTRODUCTION

FiberGLAST is a scintillating fiber detector concept instrument under development for NASA's Gamma Ray Large Area Space Telescope (GLAST) project. The detector combines a tracker section and a calorimeter section into a single detector module that will probe the high energy gamma–ray sky at energies $\gtrsim$10 MeV. The experiment concept is based on modules consisting of a converter sheet and plastic scintillating fibers arranged in orthogonal layers, and used to image the charged particles that emerge from the converter material. The fibers are read out using multi–anode photomultiplier tubes (MAPMTs). The tracker consists of 90 modules spaced with a pitch of $\sim$2 cm each, and a thickness of $\sim$0.02 radiation lengths (rl). The tracker system contains a total of 1.8 rl of converter material, and 0.4 rl of fibers, resulting in $\gtrsim$85% of 1 GeV gamma–rays converting inside the tracker. The calorimeter consists of 35 modules, each of 0.14 rl. Thus the tracker and calorimeter combined are more than 7 rl. The system is enclosed by an anticoincidence shield system composed of crossed plastic scintillator slabs, and read out with waveshifter strips coupled to photomultiplier tubes.

Because the flux level of gamma–ray sources is low, a requirement for confident source detection with high energy detectors is a large effective area. Effective area is defined as the product of the photon detection efficiency with the geometric area of the detector. Gamma–ray sources are also distributed throughout the sky, resulting in the desire for telescopes to have a wide field of view in order to observe a large number of sources. In some regions of the sky, for example, the galactic center, source density and diffuse emission is high, resulting in the requirement of good angular resolution in order to discern individual sources unambiguously. This requires an angular resolution capability on the order of 0.1 – 1.0 degrees, and depends on the energy range of the observations. The FiberGLAST instrument concept combines these capabilities by using the technology of plastic scintillating fibers as detector

Contact author: R. S. Mallozzi, *email:* Robert.Mallozzi@msfc.nasa.gov

Part of the SPIE Conference on EUV, X-Ray, and Gamma-Ray Instrumentation for Astronomy X
Denver, Colorado • July 1999 SPIE Vol. 3765 • 0277-786X/99/$10.00

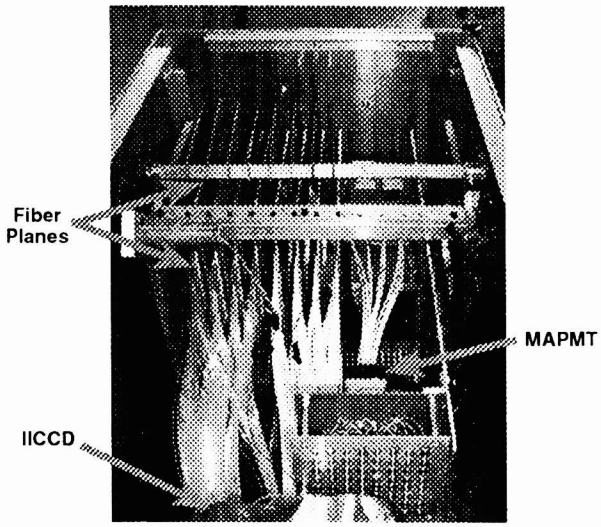

Figure 1. JLab–98 beam test apparatus with top cover removed.

elements.[1,2] Charged particles produced in the electromagnetic cascade that occurs within the detector volume are tracked throughout the active volume by the fiber planes, allowing for reconstruction of the track and derivation of the incident photon's direction. In addition, the energy deposition in the calorimeter section of the detector provides information on the incident photon's energy.

The data acquisition system contains a triggering system for forming coincidence events, and for rejecting charged particle events. Simulation studies show that this instrument concept results in an on-axis effective area of $\sim$13000 cm^2 above 25 MeV. The angular resolution is 0.33° at 1 GeV, and 2° at 100 MeV.

We have developed a small prototype instrument in order to investigate the performance of scintillating fibers, and evaluate different readout devices. This prototype was tested at the Thomas Jefferson National Laboratory. The majority of the fibers were read out using an image intensified CCD camera instead of the MAPMTs that are used in the final instrument design. In this paper, we refer to this prototype as the JLab–98 beam test apparatus. We have scheduled a second beam test (LSU–99) to be held at the Center for Advanced Microstructures and Devices at Louisiana State University in which the integrated fiber–MAPMT system will be tested. This test is scheduled to occur in 1999 July.

In sections 2 and 3 we discuss the hardware setup and facility used for the JLab-98 beam test. In section 4, we present the results for the fiber planes that were read out with the CCD camera, and in section 5 we show the results for the fiber planes read out with the MAPMT. In section 6 we discuss plans for the LSU-99 beam test, and in section 7, we present a summary and conclusions.

2. BEAM TEST HARDWARE

The JLab–98 beam test apparatus, shown in Figure 1, consisted of twelve detector planes, each of which contained arrays of scintillating blue-emitting multiclad plastic fibers. The fibers of each plane were arranged in two orthogonal layers that are denoted as the x and y layers of the plane. The plastic fibers consist of a polystyrene core with 30 μm acrylic cladding that is coated with a polymer. The detector planes were mounted on an aluminum frame assembly, and the entire apparatus was enclosed within a light tight container.

The detector planes were configured differently in order to test several hardware configurations. The forward eight planes (left side of Figure 1) were read out by a Photek MCP-340S image intensifier coupled to a Thompson TH7866 244×550 pixel CCD array, collectively denoted as the IICCD. The aft four planes were read out with a Hamamatsu R5900-064 64-anode photomultiplier tube (MAPMT). At the time of the beam test, it was not feasible to incorporate the preferred MAPMT readout system for all twelve fiber planes; thus the IICCD was used in order

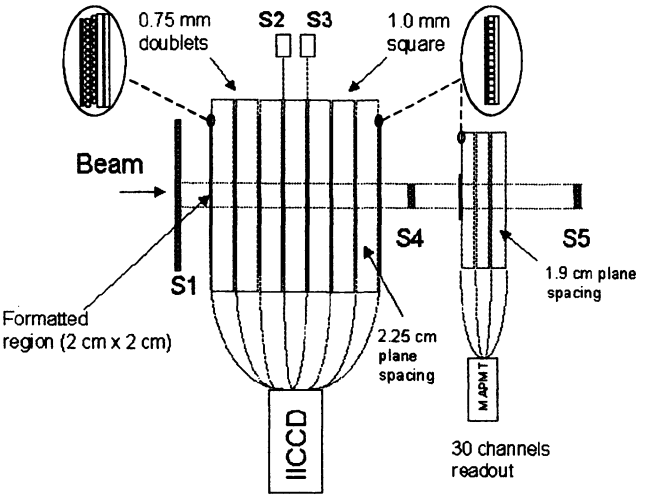

Figure 2. Schematic top view of the JLab-98 beam test apparatus showing the eight IICCD fiber planes, and the four MAPMT planes.

to facilitate the testing of the scintillation performance of the fibers. In the upcoming beam test to be performed in the summer of 1999, 20 fiber planes will be read out using a set of 20 MAPMTs. This configuration is designed as a prototype of the main FiberGLAST concept instrument tracker section. We plan to test the tracker–calorimeter combination at a later time.

A schematic of the beam test apparatus is shown in Figure 2. The beam is incident from the left. Of the eight IICCD planes, the first four had round fibers (0.75 mm diameter) arranged in a doublet configuration. Adjacent fibers were offset to allow close packing and improved tracker precision. The fibers were manufactured by Bicron Corporation, and precisely positioned with 0.9 mm pitch between adjacent centers. The remaining four planes had close-packed 1 mm^2 fibers that were produced at Washington University in St. Louis.

Each of the eight IICCD planes had 10×10 cm x-y fiber arrays mounted on an aluminum plate. The aluminum plate contained a center cut-out, and a tantalum foil of thickness 1/54 radiation length was glued directly to the fiber arrays. The spacing between each detector plane was 2.25 cm. The original design was to use the fibers over the full 100 cm^2 cut-out area, but at the time of the beam test, we were able to format a 2×2 cm region. One end of the fibers in each array was formatted onto the face of the IICCD, and the other end was sealed with an opaque, non-reflective coating.

The plastic scintillators S1 (1 cm thick), and S4 (0.63 cm thick) were placed in the front and rear of the IICCD planes as shown in the schematic, and used as anticoincidence and coincidence triggers, respectively. The non-formatted ends of the two center IICCD planes were read out with standard photomultiplier tubes (S2, S3), and used for off-line coincidence signals.

The four MAPMT planes had 30 square fibers arranged in single layer close packed arrays with 4, 6, 8, and 12 fibers per plane, with the 4-fiber plane closest to the incident beam, and the 12-fiber plane at the back of the apparatus. The planes were separated by 1.9 cm. One end of each fiber was formatted on to one of the 64 MAPMT anodes, and the other end was sealed. At the time of the test, we were able to instrument 24 of the 30 fibers onto the MAPMT. A tantalum converter foil of thickness 1/11 radiation length was glued to the first (4-fiber) plane, and a 0.63 cm plastic scintillator plate was placed behind the four planes to act as a coincidence trigger (S5) used in conjunction with an anticoincidence signal from S4 (see Figure 2).

3. JEFFERSON LAB TEST FACILITY

The beam test was held in 1998 July at the Thomas Jefferson National Laboratory Hall B, as a parasitic experiment to the CLAS instrument.[3] The accelerated electron beam was directed through a Bremsstrahlung tagging system in

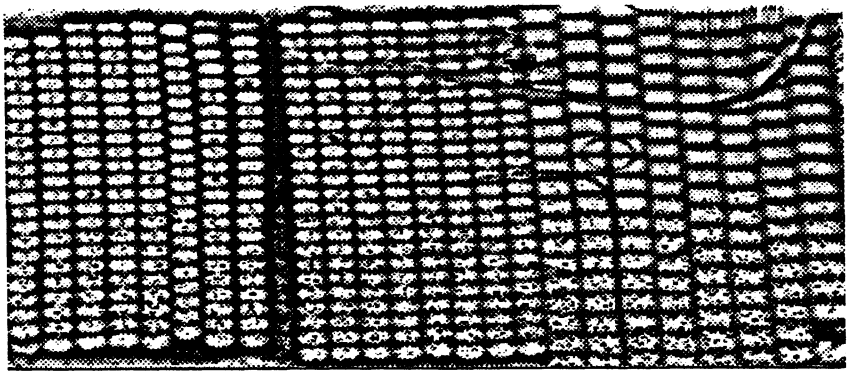

Figure 3. CCD image of 30,000 integrated events. The regions of most significant fiber response have been accentuated.

which the electrons radiate gamma rays. Approximately 1% of the gamma rays were tagged with energy and time of flight information. The photons then passed through the CLAS instrument before reaching the beam test apparatus. The tagging system provided energy information for photons in the energy range of ~0.3–2 GeV in multiple tag channels. Three tag channels (495 MeV, 1 GeV, and 1.66 GeV) were used for the fiber planes read out with the IICCD. These channels were used as a readout coincidence requirement in combination with the plastic scintillator coincidence/anticoincidence signals described in section 2. The fiber planes read out with the MAPMT did not have an energy tag line.

During two weeks of testing, the beam rate was frequently too high ($\gtrsim 10^7$ Hz) for the instrument to effectively measure individual photon events. We accumulated approximately five hours of observations during times when the beam rate was reduced by >98%, resulting in several thousand triggers.

4. IICCD DATA ANALYSIS

The eight planes of the JLab–98 beam test apparatus that were read out with the IICCD contained a total of 521 fibers. These fibers were closely packed and formatted onto the face of the CCD array. Fibers that were physically adjacent on the face of the CCD array did not necessarily correspond to adjacent fibers in the beam test apparatus, resulting in a two stage mapping process: illuminated CCD pixels were mapped to corresponding fiber indices, and the indices were then converted to real-space coordinates. Note that in this readout system, scintillation light from any single fiber can be dispersed by the image intensifier such that additional nearby pixels can be recorded as illuminated. Since there must be the complicated deconvolution process as described above in order to recover the incident photon track, the net result is that the track can be contaminated with illuminated fibers that do not conform to the true particle track. In order to reduce these artifacts, we integrated 30,000 beam test events and used the resulting image to build a CCD pixel map that contained only the most significant regions of fiber response. Regions between fibers were suppressed, resulting in lower detection efficiency. The adjusted image is shown in Figure 3. A template was created on this image, and the resulting pixel-to-fiber index map was used in the deconvolution process.

We performed detailed simulations of the beam test setup using the GEANT[4] Monte Carlo particle transport package. Non-ideal fiber efficiency was included in the simulations by randomly selecting pulse heights from a Poisson distribution. An experimentally determined mean value of 3 photoelectrons per minimum ionizing energy deposit was used, yielding a fiber efficiency of ~95%. Prior to the beam test run, the simulation data were used to develop algorithms for data analysis and reconstruction of incident photon direction. Using the new CCD pixel-to-fiber map to deconvolve the pixel data, we applied these algorithms to the IICCD data in order to estimate the angular response and fiber efficiency.

To fit incident photon tracks, the triggered events were subject to several requirements, such as the total number of fibers that were illuminated in each of the x and y projections, and the depth of the first plane that was hit. Beginning at the first plane, sets of three hit planes common to both projections were identified. These planes were

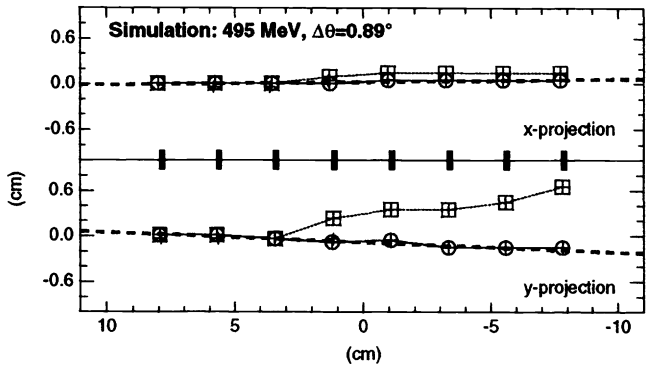

Figure 4. Simulated beam test fiber hits of 8 planes read out with the IICCD, and the resulting tracks. The incident photon direction is estimated by the heavy dashed lines.

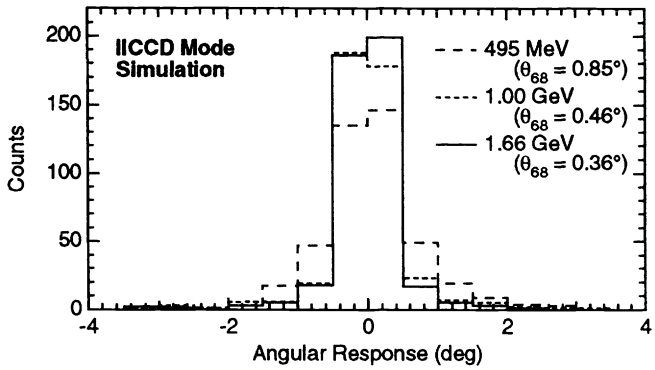

Figure 5. Simulated angular response functions for the JLab-98 beam test setup for three input photon energies.

considered as possible vertex points for a pair-conversion event. To identify a straight track through the fiber plane stack, a linear χ^2 test on sets of three track points was used to discriminate among multiple hits on individual planes. The hit yielding the lowest reduced χ^2 less than a maximum allowed value was chosen for the next track point, and the process was repeated until the end of the fiber stack was reached. The algorithm results in a primary photon track with the minimum dispersion. A second pass of the algorithm was then used to identify the secondary track, where the dispersion allowance for the track was increased from that of the primary track. Although difficult for a system with just several fiber planes, it would be straightforward to determine the most energetic track in a deep detector stack, and use this information to identify the photon primary and secondary tracks. We used only the primary track fit for the IICCD data of the JLab-98 test. For the MAPMT data (discussed below), the bisector of the primary and secondary tracks was used. Figure 4 shows an example of a simulated event and the resulting photon track.

The reconstructed incident photon directions derived from the triggered beam test events form a two-dimensional angular point spread response function about the given source location. The projection of this distribution onto one dimension for a simulated dataset is shown in Figure 5 for each of the three beam tag energies that were available. The 68% containment angles are given as a measure of the width of the distributions. As the energy increases, the distribution narrows due to smaller opening and dispersion angles for pair conversions.

Analysis of the IICCD fiber data was complicated by the relatively slow response time of the IICCD, and the large bulk of fibers outside the 2×2 cm active region. These factors resulted in a large fraction of events where single particle tracks were not clearly evident in one or both projections, even during low beam rate conditions; therefore automated event selection of the IICCD data was not possible. We manually searched several thousand events for

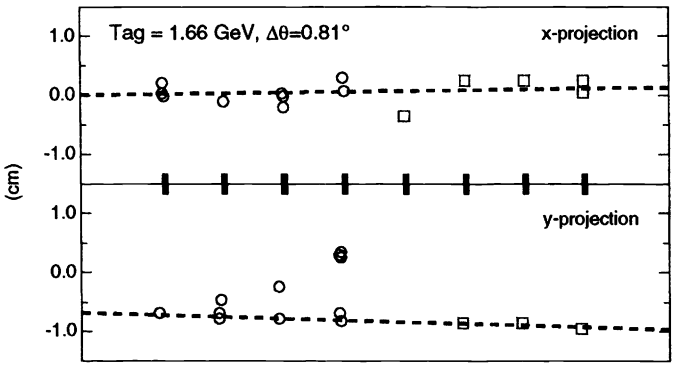

Figure 6. IICCD beam test fiber tracks. Round and square symbols (not to scale) indicate hits in the round and square fibers, respectively. The dashed lines indicate the reconstructed incident photon primary track.

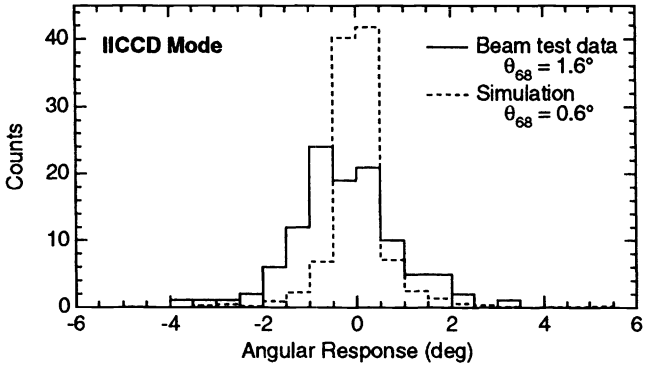

Figure 7. Angular response function for 110 IICCD events (solid line), compared with the response derived from simulations (dashed line).

candidates of single photon conversions. A sample candidate event is shown in Figure 6. As shown in the figure, contamination of nearby pixels on the CCD frame has not been completely eliminated by the mapping technique.

The tracking algorithm described above was able to reconstruct 110 of the selected candidate events. The angular response for these reconstructed events is shown in Figure 7. Also shown in the figure is the response derived from simulations. The experimental distribution is wider than the distribution of the simulations. The most likely explanations are the pixel contamination on the CCD frame, and multiple gamma–ray conversion events within the fiber planes. Both of these situations cause spurious hits near the particle path, which translate into errors in the track reconstruction process. Simulations including randomly distributed fiber hits near to the true particle tracks support this hypothesis.

5. MAPMT DATA ANALYSIS

We performed similar simulations for the fiber planes read out with the MAPMT. Incident particle tracks and angular response are shown in Figures 8 and 9. The track reconstruction algorithm described above and used for the IICCD analysis was also used in the MAPMT analysis. Comparison of Figures 5 and 9 show that the angular resolution for the MAPMT setup was less that that of the IICCD setup. This is due to the smaller number of fiber planes (4) in the MAPMT system. With four planes, it is difficult to identify the most energetic track, and hence derive the photon directional information.

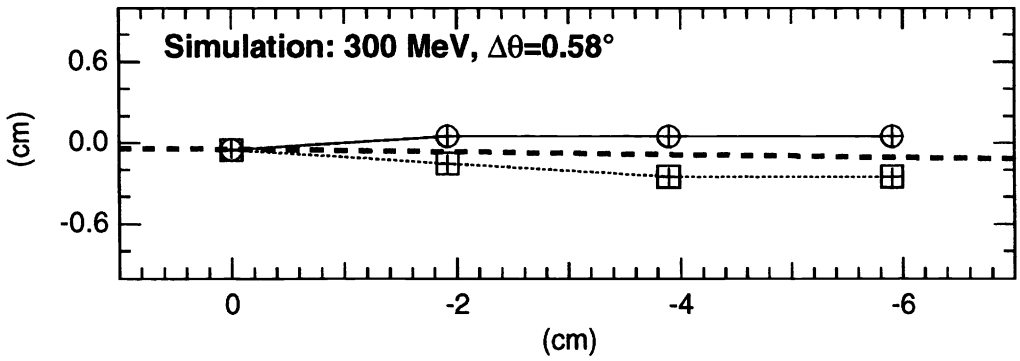

Figure 8. Simulated beam test fiber hits of planes read out with the MAPMT, and the resulting photon tracks. The incident photon direction is estimated as the weighted bisector of the primary and secondary tracks (heavy dashed line).

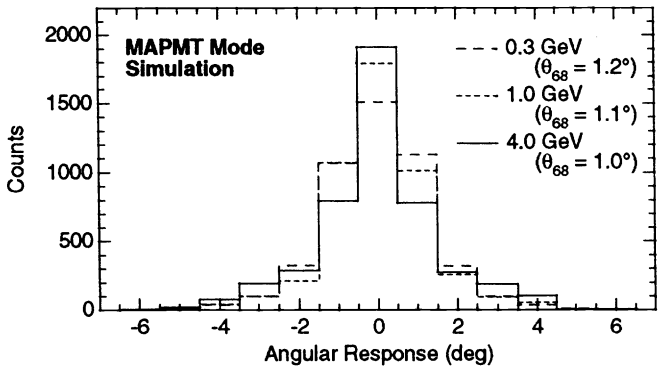

Figure 9. Simulated angular response function for the MAPMT fiber planes for three input photon energies.

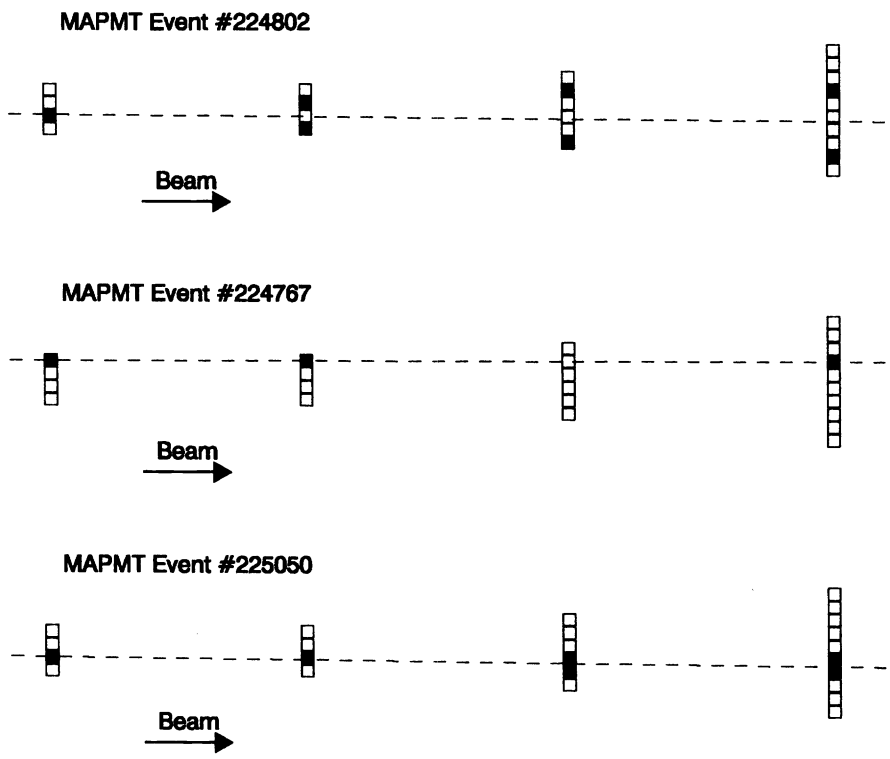

Figure 10. Three MAPMT beam test events showing the array of 24 fibers in 4 planes, with illuminated fibers shown by filled squares The dashed lines indicate the reconstructed incident photon track.

The MAPMT fiber data are relatively clean compared with the IICCD events. The fast response time helps to ensure that instrument triggers are single photon conversion events. However, the small number of fiber planes creates difficulties in identifying particle tracks. For example, conversion events can exit the system before crossing all fiber planes, resulting in fewer plane hits used as input into the track reconstruction algorithm. To filter the data, candidate events were required to have at lease one fiber hit on the plane closest to the incident beam (MAPMT plane 1), and to have hits on at least two additional planes. A set of 5582 events satisfied these criteria, 4551 of which were successfully reconstructed. Three examples of these reconstructed events are shown in Figure 10. The angular response function for these reconstructed events is shown in Figure 11. The agreement is reasonable given the uncertainty in the beam spectrum.

The detection efficiency of the MAPMT fibers was computed by counting single track events that hit the plane of interest, and its neighboring planes. The efficiency measured in this manner is 93.8% for MAPMT plane 2, and 92.4% for plane 3. The result for plane 3 is a better measure of the single particle efficiency since plane 2 is closer to the vertex, and thus has a higher probability for two photons to pass through the same fiber. This efficiency is in agreement with that measured for a setup using a Phillips MAPMT and Kuraray fibers.[5]

6. FUTURE WORK

The LSU-99 beam test instrument is composed of twenty planes of orthogonal x-y layers of scintillating fibers spaced 2 cm apart. Each x-y plane is mounted on an aluminum frame and composed of two parts: detector fibers and guard fibers. All of the guard fibers are square blue-emitting fibers with 1 mm cross-section produced by Washington University and are readout out on one end with Phillips XP2020 photomultiplier tubes. These signals are entered into the data stream to determine if fibers above, below, to the right or to the left of the detector fibers were hit. The

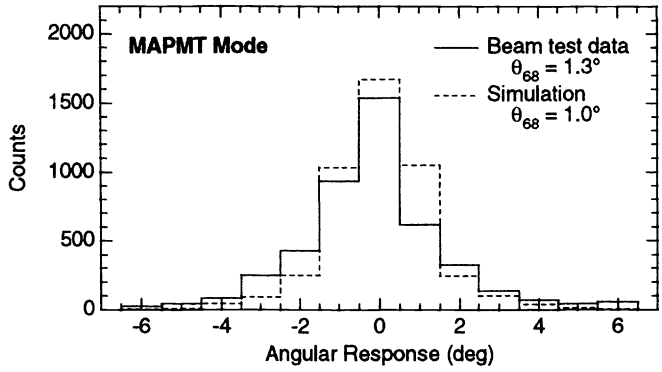

Figure 11. Angular response function for 4551 MAPMT events (solid line), compared with the response derived from simulations (dashed line).

guard fibers cover an area of 2 cm on all sides of the active area of the planes. All of the fibers within the detector volume are blue-emitting square fibers with 0.75 mm cross-section. Each plane has a thin converter plate of 0.003 in. tantalum (1/54th rl) covering the active area of the plane.

The detector system is composed of three modules. Four planes of x-y fibers are in module A, which has 16 detector fibers each in x and y with an active area of 1.44 cm^2. These detector fibers are multiclad and were manufactured in a joint effort between Bicron and Washington University. The fibers are readout on one end by Hamamatsu R5900-00-064 multianode photomultiplier tubes with one fiber on each anode. The opposite end has been diamond polished and a mirror had been vacuum deposited at a facility at Fermi National Laboratory. The detector fibers of this type are referred to as Bicron/WU/Fermi fibers. Module B contains eight planes with 32 detector fibers in the y-layer and 16 detector fibers in the x-layer for an active area of 2.88 cm^2. The first 5 layers of y-fibers are composed of Bicron/WU/Fermi fibers with the remaining 3 layers of y-fibers composed of Bicron/WU fibers with a front surface mirror coupled to the far end instead of a deposited mirror. The x-layer detector fibers manufactured at Washington University are multiclad with a front surface mirror coupled to the far end, and denoted as WU fibers. Module C contains eight layers with 64 detector fibers in the y-layer and 32 fibers in the x-layer. All of the detector fibers in module C are WU fibers. The active area of these planes is 11.52 cm^2. A schematic of the beam test apparatus is shown in Figure 12.

In front of the detector planes is a scintillator covering the entire area of the aluminum frames that is used in anticoincidence with a scintillator at the rear of the fiber planes. These scintillators can be used to trigger a read of the MAPMTs. The MAPMTs are readout with custom electronics designed and built at Washington University. Each anode signal is amplified and compared to an adjustable discriminator that fires if above threshold. The signal is high for $\sim$15 μs and the "hit" pattern is read out if coincidence has been satisfied. Coincidence can be set to be the anticoincidence of the front scintillator with the coincidence of the rear scinillator, or can be set to a self-triggered mode. The self-trigger is determined by looking for hits in n layers out of m layers, where n and m can be set to any integer. For example, a trigger might occur on any event that had 4 layers hit out of 5 consecutive layers. Louisiana State University built the self-trigger electronics.

A total of 1280 detector fibers are used in the active area and read out by 20 MAPMTs. There are 1600 guard fibers read out by 4 XP2020 PMTs. Figure 13 shows one of the electronics racks manufactured at Washington University to hold the MAPMTs and associated electronics. A single MAPMT is visible in the image. Sixty-four fibers (not shown) will be formatted onto the front face of the MAPMT and placed into the main detector volume.

Two separate beam tests will be performed with this instrument. The first will be at the Center for Advanced Microstructures and Devices, a synchrotron light source in Louisiana capable of producing photons with energy up to 1.5 GeV. This will allow us to test the self-trigger mode in several configurations. For the energy measurement, a NaI calorimeter will be placed behind the instrument and its photomultiplier tube signals will be pulse height analyzed and entered into the event data stream. The second test will occur at Thomas Jefferson National Laboratory Continuous

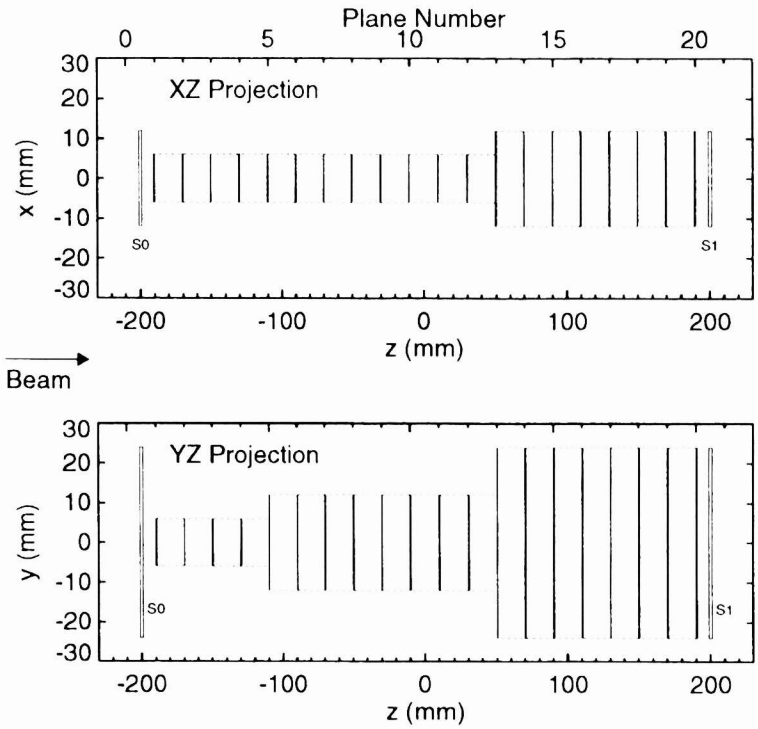

Figure 12. Planar projections of the fiber plane configuration for the LSU-99 beam test. Twenty planes with a total of 1280 fibers are read out with 20 64-anode MAPMTs. Scintillators S0 and S1 are placed at the front and back of the system, and used to trigger a readout of the MAPMTs. The fiber planes are surrounded by a set of guard fibers (not shown) used to detect interactions outside of the detector volume.

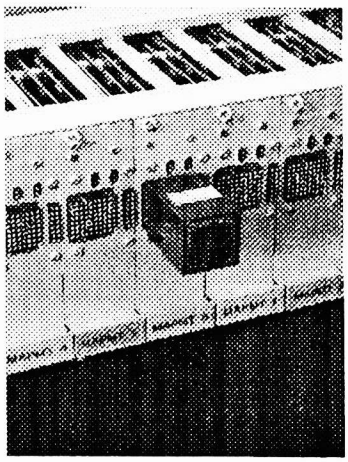

Figure 13. Electronics rack for the LSU-99 beam test, with a single MAPMT. Sixty-four scintillation fibers (not shown) will be formatted onto the front face of the MAPMT, and placed into the main detector volume.

Electron Beam Facility using the Hall B tagged photon beam. The instrument will be triggered externally in coincidence with tagged energy photons.

7. SUMMARY AND CONCLUSIONS

Our analysis indicates that the JLab-98 beam test apparatus successfully demonstrated the fiber tracking capability of the FiberGLAST instrument concept. Single gamma–ray conversion events were clearly detected and tracked even within the limited detector volume of the test. High spatial resolution was achieved by the scintillating fiber planes using two different fiber readout devices.

The advantages of the MAPMT readout system over an IICCD system were evident in the quality of the fiber hit data we recorded during the test. The single MAPMT performed exceedingly well. These devices have also recently undergone successful vibration testing at the Marshall Space Flight Center in Huntsville, Alabama to verify their flight readiness.

This test has indicated desirable refinements for future testing that we plan to incorporate in our upcoming second test at Louisiana State University in the summer of 1999. We will increase the depth of the fiber stack to 20 planes in order to measure and reconstruct single particle tracks more effectively, and increase the fiber count (effective area). This test will more closely model the final FiberGLAST concept configuration.

ACKNOWLEDGMENTS

The work was supported by NASA grant NAG5-5112. The authors would like to thank the CLAS experiment team for their consideration and help during the beam test at Jefferson National Laboratory.

REFERENCES

1. Pendleton, G. N., et al., "Development of a Gamma–Ray Scintillating Fiber Telescope for Energetic Radiation (SIFTER) with Simultaneous Tracking and Calorimetry", *SPIE Proc.*, **2806**, 164, 1996.
2. Pendleton, G. N., et al., "Scientific Capabilities of SIFTER for Discovering and Monitoring Gamma–Ray Bursts and Active Galactic Nuclei", *SPIE Proc.*, **3446**, 247, 1998.
3. Burkert, V. D. & Mecking, B. A., "Large Acceptance Detectors for Electromagnetic Nuclear Physics", *Modern Topics in Electron Scattering*, eds. B. Frois & I. Sick, World Scientific, Singapore, 1991.
4. CERN Program Library Long Writeup W5013, "GEANT-detector description and simulation tool", *CERN*, Geneva, 1993.
5. Agoritsas, V., et al., "Read-out of Scintillating Fibers Using a Weak Cross-Talk Position-Sensitive Photomultiplier", *Nucl. Inst. Meth. in Phys. A*, **A406**, 393, 1998.